J Mater Sci (2009) 44:4228–4234
DOI 10.1007/s10853-009-3520-x

Stress corrosion cracking of 2205 duplex stainless steel in H_2S–CO_2 environment

Z. Y. Liu · C. F. Dong · X. G. Li · Q. Zhi · Y. F. Cheng

Received: 10 December 2008 / Accepted: 25 April 2009 / Published online: 14 June 2009

Abstract Stress corrosion cracking (SCC) behavior of 2205 duplex stainless steel (DSS) in H_2S–CO_2 environment was investigated by electrochemical measurements, slow strain rate test (SSRT), and scanning electron microscopy (SEM) characterization. Results demonstrated that the passive current density of steel increases with the decrease of solution pH and the presence of CO_2. When solutions pH was 2.7, the steel SCC in the absence and presence of CO_2 is expected to be a hydrogen-based process, i.e., hydrogen-induced cracking (HIC) dominates the SCC of the steel. The presence of CO_2 in solution does not affect the fracture mechanism. However, the SCC susceptibility is enhanced when the solution is saturated simultaneously with H_2S and CO_2. With elevation of solution pH to 4.5, the hydrogen evolution is inhibited, and dissolution is involved in cracking process. Even in the presence of CO_2, the additional cathodic reduction of H_2CO_3 would enhance the anodic reaction rate. Therefore, in addition to the hydrogen effect, anodic dissolution plays an important role in SCC of duplex stainless steel at solution pH of 4.5.

Introduction

Sulfide stress corrosion cracking (SCC) has been identified as one of essential threats to the componential integrity in petroleum and petrochemical industries [1–4]. In recent years, the continuously increasing energy demands drive the exploration of deep, high H_2S-, and CO_2-containing oil and gas wells [5], where high strength steels and stainless steels are required to resist high stress and highly corrosive environment [6–12].

The 2205 duplex stainless steels (DSS) becomes a promising candidate material used in H_2S environment due to its excellent mechanical behavior and high corrosion resistance. Extensive work has been conducted to investigate SCC behavior of 2205 DSS under a variety of environmental conditions. For example, hydrogen embrittlement (HE) and SCC of duplex stainless steel was studied in either NACE TM-0177 standard solution [13] or in simulated service conditions [4, 14–17]. Tsai and Chen [16] demonstrated that 2205 DSS was immune to SCC in a concentrated NaCl solution up to 26 wt% concentration in a near neutral pH condition. However, 2205 DSS undergoes HE in hydrogen-charging conditions, such as cathodic polarization or in the presence of hydrogen sulfide [18]. Furthermore, Luu et al. [19] and Owczarek et al. [20] reported that the ferritic phase in 2205 DSS is more susceptible to HE and hydrogen-induced cracking (HIC) under hydrogen charging. El-Yazgi and Hardie [4] found that SCC of duplex and super-duplex stainless steels occurred in a wide temperature range in sour environment.

To date, research has been focused on SCC of 2205 DSS in H_2S- or CO_2-containing conditions. There has been limited work conducted under the environmental condition where the interaction of CO_2 and H_2S plays an essential role in SCC of duplex stainless steel. Furthermore, a mechanistic effect of solution pH on SCC of DSS has remained unclear. Thus, this work is an expansion of some of previous research.

Z. Y. Liu · C. F. Dong · X. G. Li (✉) · Q. Zhi
Corrosion and Protection Center, University of Science and Technology Beijing, Beijing 100083, China
e-mail: lixiaogang99@263.net

Y. F. Cheng (✉)
Department of Mechanical & Manufacturing Engineering, University of Calgary, Calgary, AB T2N 1N4, Canada
e-mail: fcheng@ucalgary.ca

In this work, electrochemical measurement, slow strain rate test (SSRT), and surface analysis technique were combined to investigate the effects of pH, CO_2, and stress on SCC susceptibility of 2205 DSS in H_2S-containing environment. The interaction of various affecting factors in SCC of DSS was analyzed. It is anticipated that this research provides an essential insight into the mechanism of SCC of DSS in H_2S- and CO_2-containing conditions as well as the role of solution pH in the steel SCC.

Experimental procedure

Specimens used in this work were cut from a commercial cold-rolling 2205 DSS plate, with the chemical composition (wt%): C 0.029, Si 0.59, Mn 1.20, Cr 22.57, Ni 4.63, Mo 2.62, N 0.13, S 0.0043, P 0.029, and Fe balance. Electrodes for electrochemical measurements were ground to 600 grit emery papers on all faces. The unexposed edges were coated with a masking paint to prevent crevice corrosion between the epoxy mount and the electrode. The specimens were embedded in epoxy resin manufactured by LECO leaving a working area of 1.0 cm^2. The working surface was subsequently polished with 3 and 1 μm diamond pastes, cleaned by distilled water and methanol. The specimens for SSRT, made according to GB T15970 specification [21], were covered with LECO epoxy resin, leaving a working area of 2.4 cm^2. The working surface of specimen was subsequently polished with 800 and 1,000 grit emery papers, cleaned by distilled water and acetone.

A metallographic examination of 2205 DSS showed that it contained a duplex ferritic–austenitic microstructure after chemically etching in solution of 20 mL HCl, 20 mL H_2O, and 5 g $CuSO_4{\cdot}5H_2O$, as seen in Fig. 1. SSRT test was performed in air to obtain the mechanical properties of the steel: yield strength ($\sigma_{0.2}$) 506 MPa, ultimate strength (σ_b) 717 MPa, elongation rate (δ) 40.5%, and reduction-in-area (Ψ) 67.9%.

The basic test solution was NACE TM0177-1996 solution of 5% NaCl + 0.5% CH_3COOH + saturated H_2S (pH = 2.7), where the saturated H_2S concentration in the solution was about 3,200 ppm. Three other solutions were prepared to investigate the effects of solution pH and CO_2 concentration: 5% NaCl + 0.5% CH_3COOH + saturated H_2S (pH 4.5), 5% NaCl + 0.5% CH_3COOH + saturated H_2S + saturated CO_2 (pH 2.7), and 5% NaCl + 0.5% CH_3COOH + saturated H_2S + saturated CO_2 (pH 4.5). A solution of 5% NaOH was used to adjust pH values of the test solutions. The saturated CO_2 concentration in solution was approximately 5,000 ppm. All solutions were deaerated with highly pure nitrogen gas (99.99%) prior to tests.

Two loading methods were used to study SCC of stressed steel specimen. The first one was to prepare a U-bent specimen, based on ASTM G30 [22], to obtain a static stress, with the axial direction of the outer bent surface paralleling to the rolling direction. U-bent specimens were soaked in the test solutions for 720 h, and then cleaned and examined by an optical microscopy and scanning electron microscopy (SEM). The second method was to use SSRT technique to create a dynamic tensile loading at a strain rate of 1×10^{-6} s^{-1}. SSRTs were performed on a WDML-30KN Materials Test System. All tensile specimens were ground parallel to the tension direction to 800 grit emery papers. The test was performed at corrosion potential and ambient temperature (about 20 °C).

Potentiodynamic polarization curve measurements were carried out through a 2273 electrochemical system by a three-electrode cell, with an unstressed 2205 DSS specimen as working electrode, a saturated calomel electrode as reference electrode, and a platinum plate as counter electrode. Polarization range was from −500 mV to 2,500 mV (vs. corrosion potential) at a potential sweep rate of 1 mV/s. The tests were conducted at room temperature (~22 °C).

Fracture surface of tensile specimens after SSRT and the corrosion morphology of working electrodes after electrochemical tests were observed by SEM.

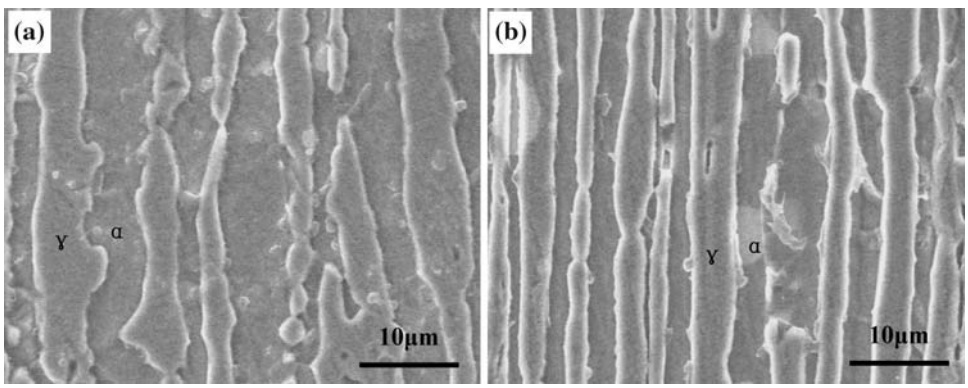

Fig. 1 Microstructure of 2205 duplex stainless steel. **a** Parallel to rolling plane and **b** normal to rolling plane

Results

Electrochemical measurements

Figure 2 shows the polarization curves measured on 2205 DSS electrode in solutions saturating with H_2S. It is seen that passivity was achieved on steel in all solutions. While there was little change of corrosion potential in various solutions, as shown in Fig. 2b in detail, the passive current density differs from each other remarkably. In general, an increase in solution pH decreased the passive current density, and purging CO_2 in solution increased the current density. Moreover, there was an active–passive transition range for curves measured at pH 2.7 with and without CO_2. However, in solutions with pH 4.5, the passive current density was relatively stable, without an apparent active–passive transition.

U-bent specimen soaking test

For specimens soaked in solutions without CO_2, there was no crack found on the outer surface the specimen, and the specimen remained shiny. However, for those soaked in pH 2.7 and 4.5 solutions with CO_2, although there was no crack observed, the surface of the specimen became gray and remained shiny, respectively. Figure 3 shows the SEM observation of the specimen soaked in pH 2.7, H_2S-saturated solution without and with CO_2. It is seen that there was no corrosion sign on specimen soaked in CO_2-free solution, while the specimen soaked in CO_2-containing solution contained a number of transgranular micro-cracks that were transverse to the loading direction on the surface.

SSRTs

Typical stress–strain curves obtained by SSRT on 2205 DSS specimen in various solutions are shown in Fig. 4. Generally, there was a lower elongation-to-rupture in solutions with a lower pH than that in a higher pH solution. Furthermore, the presence of CO_2 in solution decreased elongation remarkably.

Furthermore, the susceptibility of steel to SCC in different solutions was determined by reduction-in-area factor (I_Ψ), as shown in Fig. 5. I_Ψ was defined as:

$$I_\Psi = \left(1 - \frac{\Psi_S}{\Psi_0}\right) \times 100\%, \quad (1)$$

where Ψ_S and Ψ_0 were reduction-in-areas measured in solution and in air, respectively. It is seen from Fig. 5 that with the decrease of pH value, I_Ψ increased significantly. Moreover, I_Ψ determined in CO_2-containing solution was higher than that obtained in CO_2-free solution at individual pH. Since I_Ψ was a ductility-loss parameter [6, 7], it was apparent that the SCC susceptibility of 2205 DSS increased with the decreasing solution pH and the presence of CO_2 at individual pH value. The result was consistent with that analyzed by elongation-to-rupture.

SEM observation of fracture surface and cracks

No crack was observed on the circumferential surface of specimens tested in pH 4.5 solutions without and with CO_2. For specimens tested in solutions with pH 2.7, cracks were found in both solutions with and without CO_2, as shown in Fig. 6.

Figure 7 shows the SEM pictures at crack-tip area and the crack initial zone in pH 2.7 solution without and with CO_2. It is seen that the fracture morphology of specimen in both solutions was similar. An island-and-ravine morphology, as shown in Fig. 7b, d, was observed, where the ruptured γ-phase was the island, and δ-phase was corroded along crack wall and left ravine surrounding the γ-phase island.

Figure 8 shows the fracture surfaces of specimens tested in pH 2.7 and 4.5 solutions with and without CO_2. In pH 2.7 solutions, the fracture showed a brittle feature (Fig. 8a, c),

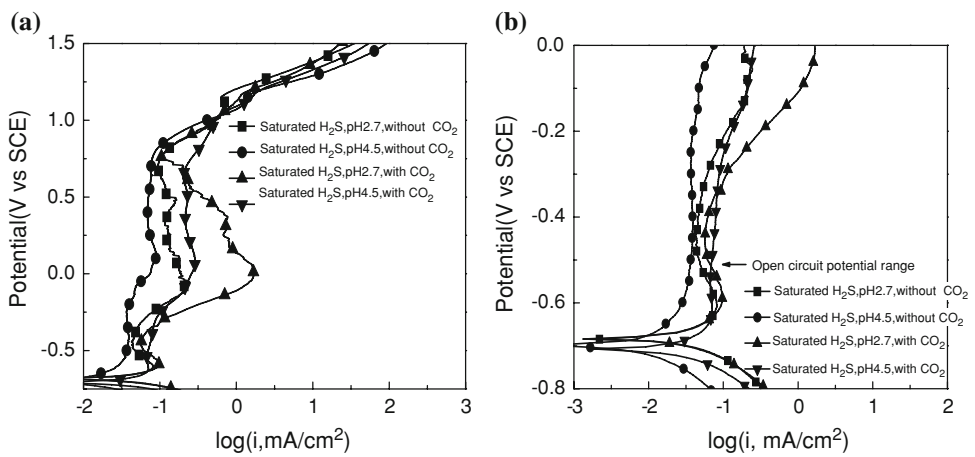

Fig. 2 Potentiodynamic curves **a** of 2205 DSS in various solutions and **b** detailed view of polarization curves around corrosion potential

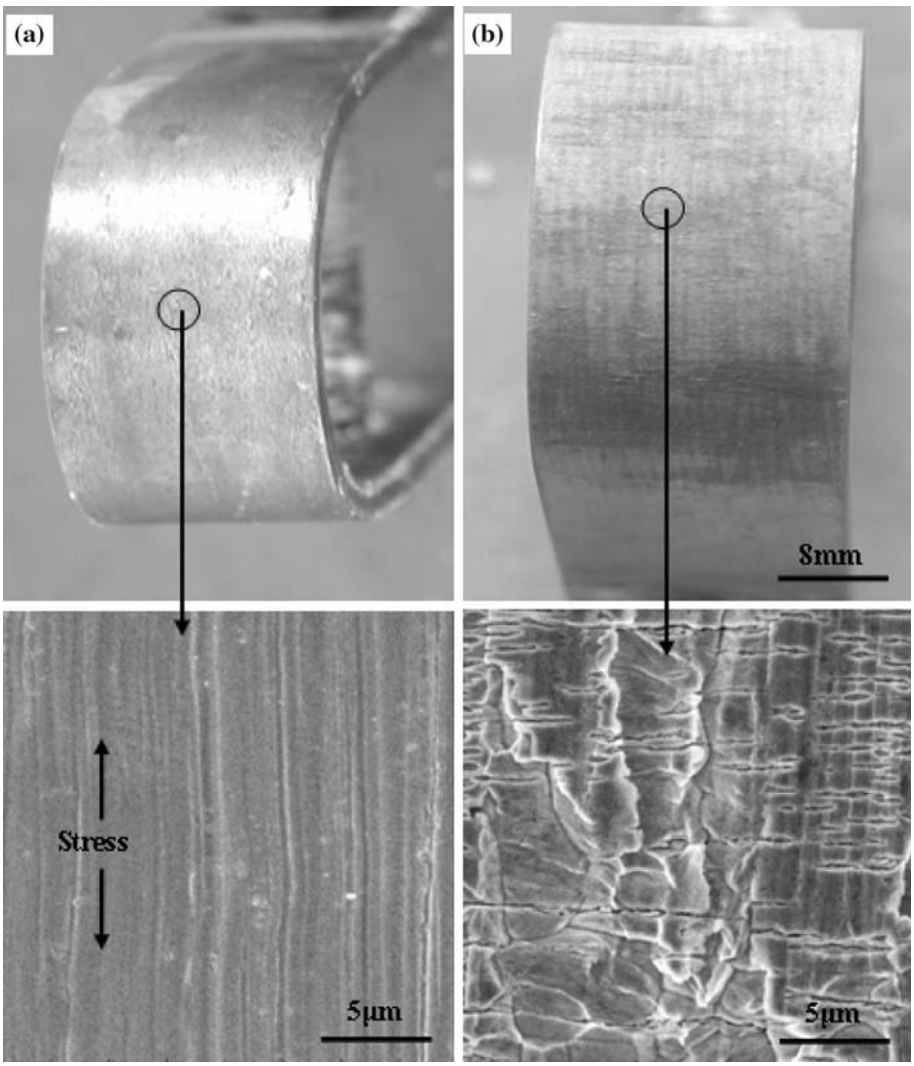

Fig. 3 SEM images of morphology of U-type bent specimens soaked in saturated H_2S solutions (pH = 2.7) for 720 h **a** without CO_2 and **b** with CO_2

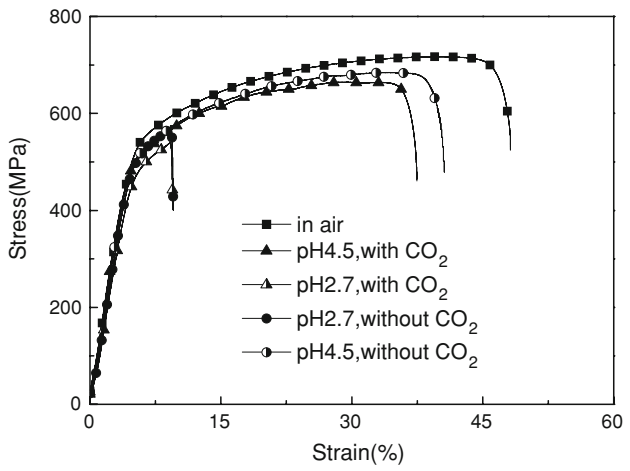

Fig. 4 Stress–strain curves of 2205 DSS in various solutions

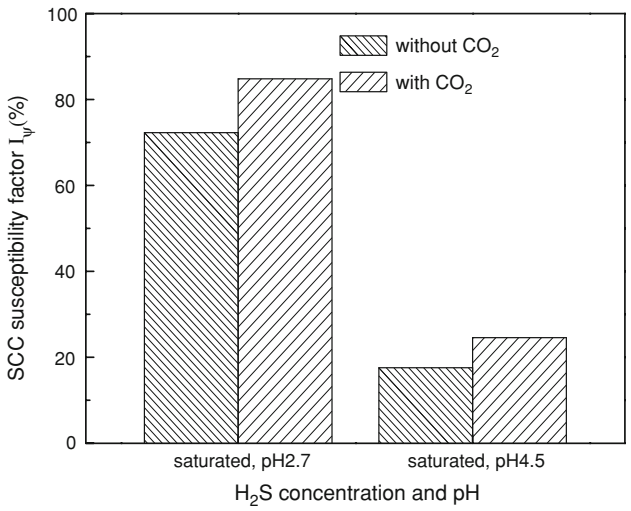

Fig. 5 SCC susceptibilities in terms of reduction-in-area in various solutions

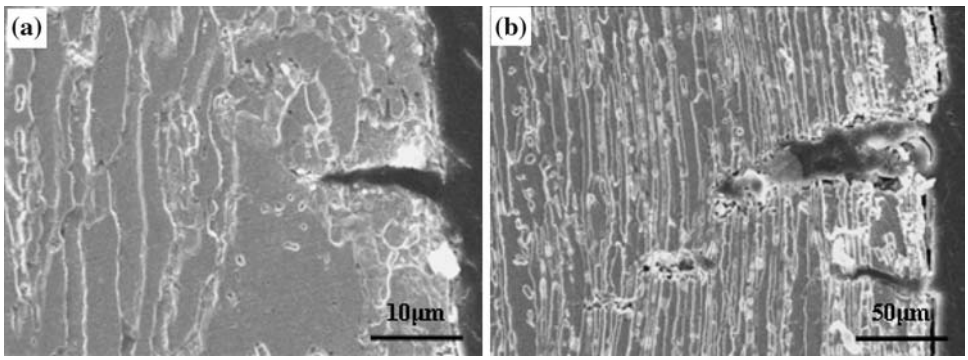

Fig. 6 SEM views of side surface of 2205 DSS specimens tested in pH 2.7 solutions **a** without and **b** with CO_2

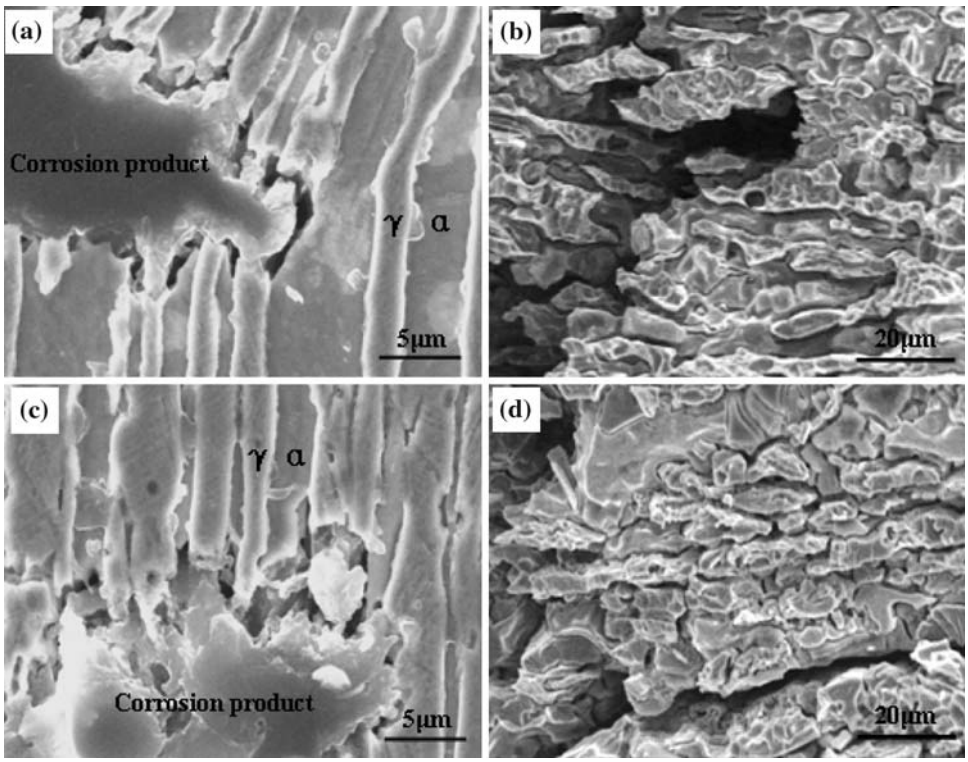

Fig. 7 SEM views of cross-section of crack-tip (**a**, **c**) and crack zone (**b**, **d**) on fracture surface. **a** and **b** were obtained in solutions without CO_2 and pH 2.7, **c** and **d** were obtained in solutions with CO_2 and pH 2.7

while the fracture surface contained ductile dimples in pH 4.5 solutions (Fig. 8b, d). The presence of CO_2 would not alter the fracture feature.

Discussion

Electrochemical corrosion mechanism of DSS in H_2S–CO_2 solution

The cathodic and anodic reactions of 2205 DSS in the deaerated, acidic (pH < 3), H_2S solution are primarily reduction of hydrogen ions and the oxidation of steel to form iron sulfide [23]:

$$H^+ + e \rightarrow H, \quad (2)$$

$$H_2S \Leftrightarrow H^+ + HS^- \Leftrightarrow 2H^+ + S^{2-}, \quad (3)$$

$$Fe + S^{2-} \rightarrow FeS \downarrow + 2e, \quad (4)$$

$$Fe + HS^- \rightarrow FeS \downarrow + H^+ + 2e. \quad (5)$$

Reactions 4 and 5 would generate a FeS layer on the electrode surface. The FeS film was somewhat capable of blocking further dissolution of steel. At an elevated pH, the formation of FeS film is favored, resulting in a decreasing anodic current density, as shown in Fig. 2.

Furthermore, as a cathodic depolarizer, FeS stimulates the reduction of H^+ into H that could penetrate into steel substrate:

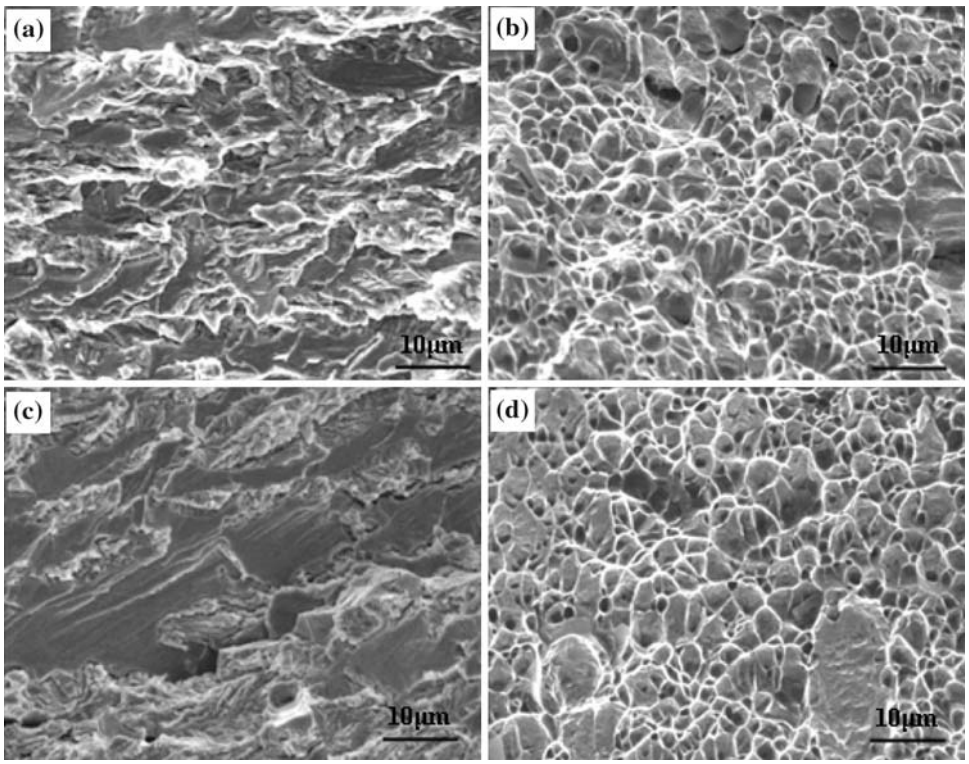

Fig. 8 Fracture surfaces of SSRT specimens in solutions: **a** pH 2.7 without CO_2, **b** pH 4.5 without CO_2, **c** pH 2.7 with CO_2 and **d** pH 4.5 with CO_2

$$H_2S_{sol} \rightleftharpoons H_2S_{ad}, \quad (6)$$

$$H_2S_{ad} + e \rightleftharpoons H_{ad} + HS^-_{ad}, \quad (7)$$

$$HS^-_{ad} + e \rightleftharpoons H_{ad} + S^{2-}_{ad}, \quad (8)$$

$$H_{ad} + H_{ad} \rightarrow H_2, \quad (9)$$

$$H_{ads} \rightarrow H_{abs}. \quad (10)$$

In the presence of CO_2, the dissolved CO_2 achieves an equilibrium with water [24, 25]:

$$CO_2 + H_2O \Leftrightarrow H_2CO_3, \quad (11)$$

$$H_2CO_3 \Leftrightarrow H^+ + HCO^-_3, \quad (12)$$

$$HCO^-_3 \Leftrightarrow H^+ + CO^{2-}_3. \quad (13)$$

Apparently, dissociation of H_2CO_3 serves as an additional source of H^+, contributing to an enhanced cathodic reaction [26]. In low pH solution, e.g., pH 2.7, reduction of hydrogen ions is still the dominant cathodic reaction. Reduction of H_2CO_3 and thus the formation of $FeCO_3$ corrosion product film are thermodynamically unfavorable [27]. As demonstrated in Fig. 2, the enhanced cathodic reaction results in the increase of anodic current density in the presence of CO_2 in the solution.

When solution pH is elevated to 4.5, the presence of CO_2 results in an additional cathodic reduction reaction of H_2CO_3:

$$H_2CO_3 + e \rightarrow HCO^-_3 + H. \quad (14)$$

Therefore, the anodic dissolution of steel is enhanced.

In summary, although the presence of CO_2 in solution would enhance the anodic current density of steel, the mechanisms underlying are quite different at low and intermediate pH solutions, which are featured with reduction of hydrogen ions and carbonate acid, respectively.

SCC of 2205 DSS in H_2S/CO_2 solutions

The present work shows that the susceptibility of 2205 DSS to SCC in saturated H_2S solution increases when the solution pH decreases and/or CO_2 is purged in the solution (Figs. 4, 5). In solutions of pH 2.7, SCC of the steel in the absence and presence of CO_2 is expected to be a hydrogen-based process, i.e., HIC dominates the SCC of the steel. As analyzed, the dominant cathodic reaction in low pH solution is hydrogen evolution. Moreover, sulfide compounds contained in the solution serve as a poisonous effect to promote hydrogen entry into the steel. The river-bed pattern observed in fracture surface of the specimens (Fig. 8a, c) is typical of that resulted from HIC. Furthermore, when solution pH is sufficiently low, e.g., pH 2.7 in this work, the presence of CO_2 in the solution does not alter the fracture mechanism of HIC. Cracks could be initiated no matter if CO_2 is present in the system, as seen in Fig. 6. However, the SCC susceptibility is enhanced when the test solution contains simultaneously H_2S and CO_2 (Fig. 5), which is attributed to the enhanced hydrogen evolution. Due to dissociation of H_2CO_3, additional hydrogen ions are generated and then reduced to produce hydrogen atoms,

contribute to the increasing HIC susceptibility of the steel upon hydrogen permeation.

With elevation of solution pH to 4.5, the hydrogen evolution is inhibited, and dissolution is involved in cracking process. Therefore, in addition to the hydrogen effect, anodic dissolution plays an important role in SCC of steel. As seen in Fig. 8b, d, the fracture morphology is not completely brittle any more, and ductile dimples are observed due to the decreasing hydrogen-induced embrittlement accompanying with the dissolution effect.

In general, steels with a two-phase microstructure, such as austenite and ferrite, are more prone to hydrogen-induced embrittlement. In 2205 DSS, there are two phases, austenite (γ-Fe, face centered cubic crystals) and ferrite (δ-Fe, body centered cubic crystals), with approximately 50% volume/volume fraction for each phase. The δ-phase usually exhibits high strength and resistance to Cl^- attack, and γ-Fe can release stress concentration and block crack propagation beyond α-Fe. Consequently, there is a high resistance to SCC of 2205 DSS [4]. However, in case of hydrogen entry into steel, the steel becomes very susceptible to HIC. Since the hydrogen diffusion coefficient in γ-Fe is low, hydrogen is mainly trapped in irregularities in γ-Fe [10, 15], and diffuse mainly through the δ-Fe grid [28].

Conclusions

The passive current density of 2205 DSS increases with the decrease of solution pH and the presence of CO_2 in aerated, H_2S-containing solution. In low pH solution, e.g., pH 2.7, the increasing anodic current density is due to cathodic reduction of additional hydrogen ions generated due to dissociation of H_2CO_3. With elevation of solution pH to 4.5, reduction of H_2CO_3 becomes thermodynamically possible, providing an additional cathodic reduction and resulting in the increase of anodic current density.

In solutions with low pH, e.g., pH 2.7, SCC of the steel in the absence and presence of CO_2 is expected to be a hydrogen-based process, i.e., HIC dominates the SCC of the steel. When solution pH is sufficiently low, the presence of CO_2 in the solution does not affect the fracture mechanism. However, the SCC susceptibility is enhanced when the test solution is saturated simultaneously with H_2S and CO_2.

With elevation of solution pH to 4.5, the hydrogen evolution is inhibited, and dissolution is involved in cracking process. Even in the presence of CO_2, the additional cathodic reduction of H_2CO_3 enhances the anodic reaction rate. Therefore, in addition to the hydrogen effect, anodic dissolution plays an important role in SCC of steel.

Acknowledgements This work was supported by Chinese National Science and Technology Infrastructure Platforms Construction Project (No. 2005DKA10400), and Canada Research Chairs Program.

References

1. Oltra R, Desestret A, Mirabal E, Bizouard JP (1987) Corros Sci 27:1251
2. Van Gelder K, Erlings JG, Damen JWM, Visser A (1987) Corros Sci 27:1271
3. Barteri M, Mancia F, Tama A, Montagna G (1987) Corros Sci 27:1239
4. El-Yazgi AA, Hardie D (1998) Corros Sci 40:909
5. Liu ZD, Huang LM, Gu T (2006) Mater Perform 45:52
6. Turnbull A, Nimmo B (2005) Corros Eng Sci Technol 40:103
7. Turnbull A, Griffiths A (2003) Corros Eng Sci Technol 38:21
8. Moura V, Kina AY, Tavares SSM, Lima LD, Mainier FB (2008) J Mater Sci 43:536. doi:10.1007/s10853-007-1785-5
9. Vasconcelos IF, Tavares SSM, Reis FEU, Hamilton FG (2009) J Mater Sci 44:293. doi:10.1007/s10853-008-3064-5
10. Umoren S, Obot I, Obi-Egbedi N (2009) J Mater Sci 44:274. doi:10.1007/s10853-008-3045-8
11. Xia SA, Zhou BX, Chen WJ (2008) J Mater Sci 43:2990. doi:10.1007/s10853-007-2164-7
12. Radiguet B, Etienne A, Pareige P, Sauvag X, Valiev R (2008) J Mater Sci 43:7338. doi:10.1007/s10853-008-2875-8
13. Sozanska M, Kłyk-Spyra K (2006) Mater Charact 56:399
14. De Moraes FD, Bastian FL, Ponciano JA (2005) Corros Sci 47:1325
15. Zakroczymski T, Owczarek E (2002) Acta Mater 50:2701
16. Tsai WT, Chen MS (2000) Corros Sci 42:545
17. Tsay LW, Young MC, Shin CS, Chan SLI (2007) Fatigue Fract Eng Mater Struct 30:1228
18. Tsai ST, Yen KP, Shin HC (1998) Corros Sci 40:281
19. Luu WC, Liu PW, Wu JK (2002) Corros Sci 44:1783
20. Owczarek K, Zakroczymski T (2000) Acta Mater 48:3059
21. Chinese National Standard for Stress Corrosion Cracking Tests, GB T15970, 2007
22. ASTM G 30-97 (2003) In: Annual Book of ASTM Standards, vol 03.02. ASTM International, West Conshohocken, PA
23. Mancia F (1987) Corros Sci 27:1225
24. Davies DH, Burstein GT (1980) Corrosion 36:416
25. Ren CQ, Liu DX, Bai ZQ, Li T (2005) Mater Chem Phys 93:305
26. Nesic S, Nordsveen M, Nyborg R, Stangeland A (2001) In: Corrosion/2001, Paper No. 01040, Nace, Houston
27. Nesic S, Postlethwaite J, Olsen S (1996) Corrosion 52:280
28. Videm K, Kvarekval J (1995) Corrosion 51:260